Standardized Benchmark of Historical Compound Wind and Solar Energy Droughts Across the Continental United States

Cameron Bracken[a,1], Nathalie Voisin[a,2], Casey D. Burleyson[a,3], Allison M. Campbell[a,4], Z. Jason Hou[a,5], Daniel Broman[a,6]

[a] Pacific Northwest National Laboratory
902 Battelle Boulevard, Richland, WA, 99352, USA.

This is a non-peer reviewed preprint submitted to EarthArXiv. The manuscript was submitted for publication in *Renewable Energy.* Please contact the lead author with any comments or questions.

[1]cameron.bracken@pnnl.gov
[2]nathalie.voisin@pnnl.gov
[3]casey.burleyson@pnnl.gov
[4]allison.m.campbell@pnnl.gov
[5]zhangshuan.hou@pnnl.gov
[6]daniel.broman@pnnl.gov

Standardized Benchmark of Historical Compound Wind and Solar Energy Droughts Across the Continental United States

Cameron Bracken[a], Nathalie Voisin[a], Casey D. Burleyson[a], Allison M. Campbell[a], Z. Jason Hou[a], Daniel Broman[a]

[a] *Pacific Northwest National Laboratory, 902 Battelle Boulevard, Richland, 99352, WA, USA*

Abstract

As we move towards a decarbonized grid, reliance on weather-dependent energy increases as does exposure to prolonged natural resource shortages known as energy droughts. Compound energy droughts occur when two or more predominant renewable energy sources simultaneously are in drought conditions. In this study we present a methodology and dataset for examining compound wind and solar energy droughts as well as the first standardized benchmark of energy droughts across the Continental United States (CONUS) for a 2020 infrastructure. Using a recently developed dataset of simulated hourly plant level generation which includes thousands of wind and solar plants, we examine the frequency, duration, magnitude, and seasonality of energy droughts at a variety of temporal and spatial scales. Results are presented for 15 Balancing Authorities (BAs), regions of the U.S. power grid where wind and solar are must-take resources by the power grid and must be balanced. Compound wind and solar droughts are shown to have distinct spatial and temporal patterns across the CONUS. BA-level load is also included in the drought analysis to quantify events where high load is coincident with wind and solar droughts. We find that energy drought characteristics are regional and the longest droughts can last from 16 to 37 continuous hours, and up to 6 days. The longest hourly energy droughts occur in Texas while the longest daily droughts occur in California. Compound energy drought events that include load are more severe on average compared to events that involve only wind and solar. In addition, we find that compound high load events occur more often during compound wind and solar droughts that would be expected due to chance. The insights obtained from these findings and the summarized characteristics of energy drought provide valuable guidance on grid planning and storage sizing at the regional scale.

Keywords: energy droughts, compound energy droughts, renewable energy

1. Introduction

Hydrologic droughts bring to mind dry soils, low flows and withering crops spanning large geographic regions, lasting months or years, affecting entire populations. While energy droughts from renewable sources occur on a much shorter time scale, they can span similarly large geographic regions as both are fundamentally driven by meteorology. Energy droughts result in energy price spikes that cascade into large-scale power grid impacts such as blackouts, brownouts, and acute carbon emissions from thermoelectric plants that provide for the lost generation [1, 2, 3]. As intermittent renewables continue their rapid expansion in a decarbonized grid, the impacts of energy droughts on the power grid's reliability, economic performance and greenhouse gas emissions is increasing and thus needs more understanding [4].

Although transmissions can alleviate the stress of a drought of a predominant renewable resource in one particular region [5, 6], coincident droughts that involve multiple renewable resources such as wind, solar and hydro are of particular concern for their potential grid impacts. These coincident, or compound energy droughts can be defined for any two or more variables, though typically wind and solar are of the most interest due to their extensive adoption and growing integration into grids across the world [7, 8, 9, 10, 2, 11, 12]. In Germany, these compound drought events are common enough that the word dunkelflaute has come to describe their impact to the grid [13].

Drought events involving only sources of energy production are known as energy production droughts [2]. Energy supply droughts involve use of load, typically determined from the net load or the load after subtracting wind and solar production. In some cases, energy supply droughts may be statistically significant but have no actual impact on the grid. For example, during a period of high hydro generation, wind and solar could be in drought conditions yet still be curtailed, giving the drought little or no impact. By including load in the definition of drought we are able to assess the frequency, duration, and magnitude of drought events that have a greater chance of impacting the grid.

Previous studies have focused on general meteorological drivers for energy droughts [14, 1, 15, 16, 17], or specifically on the reliability of complementary renewable systems [18, 19, 20]. Other studies have looked at energy droughts and the complementarity of wind and solar in Europe [21, 7, 22, 23, 10, 2, 24, 25, 1, 26, 11], Latin America [27, 8] and Africa [28]. Relatively few studies have focused on North America. [12] examined weekly droughts for a region encompassing most of western North America, finding that compound wind and solar droughts were most likely to occur in the winter under specific atmospheric circulation patterns. [29] demonstrated summertime meteorological drivers of relevance to renewable energy supply and demand. [30] examined wind and solar energy droughts separately for California and the Western Interconnection, finding that few daily-timescale droughts last longer than 7 days. [31] developed a space-time simulation model that generates fields of hydroclimatic data used in energy drought analysis, and applied their model to Texas.

Although energy droughts have been a focus in the aformentioned studies, none of them employ a standardized definition of drought. There are variations in the time scales applied, drought thresholds, and seasonality considerations when defining droughts. The lack of standardization prevents the ability to measure energy droughts and link them to their impact on the power grid as well as understanding the opportunities to design and site short to long term duration storage technologies. In this paper we adopt the standardized energy drought indices introduced by [32] and inspired by the indices used in hydrology and climatology [33].

The time scale of a drought is strongly related to the frequency and duration of drought events [33]. Most previous studies use a single time scale to discuss energy droughts (typically 1-day or 1-week). In this study we look at several time scales ranging from 1-hour to 5-days specifically designed around the management of hydropower and other potential storage resources. Energy drought studies typically define droughts as consecutive periods of low or no production. This definition is complicated somewhat when looking at sub-daily scales due to regular overnight periods with no solar production. Some special consideration for these periods is necessary.

In this study we examine energy droughts across the Continental US (CONUS) at the Balancing Authority (BA) scale. The wind and solar are considered "must-take" by the power grid at the BA scale. Because of the intermittency, solar and wind are also considered non-dispatchable through the transmission system. This scale is similar to countries and provinces and is strategic in that wind, solar and load need to be balanced prior to understanding transmission needs. This spatial scale was chosen for its application to future studies examining storage siting, sizing and operational guidance to accommodate droughts and address reliability requirements in conjunction with the role of transmission. The goals of this study are to (1) develop the first CONUS-scale assessment and benchmark of energy droughts for the current (2020) infrastructure of wind and solar power plants and (2) characterize the frequency, duration, and intensity of energy droughts including their temporal and spatial distribution to inform power grid planning studies – specifically storage versus transmission in long term planning studies. By utilizing actual wind and solar plant configuration data from the U.S. Energy Information Administration (EIA) we get a view that is as representative as possible to actual conditions. The analysis is based on the contemporary (2020) wind and solar fleet and 40 years of historical weather (1980-2019). Future studies will look at future infrastructure and weather conditions.

2. Data

2.1. Wind and Solar Generation Data

We utilized the simulated plant level solar and wind generation data produced as part of [34]. The dataset includes hourly wind and solar generation for all EIA-860 2020 plant locations [35] using weather from 1980-2019 [36]. The reader is referred to that paper for full details, but a brief summary of the approach is summarized here.

The wind and solar generation is based on meteorological data from the Thermodynamic Global Warming (TGW) simulation data [37, 38]. TGW is dynamically downscaled based on ERA5 boundary conditions [39]. The dataset includes historical simulations and future projections, but for this study we only utilized the historical data (1980-2019). All meteorological variables are available at 1/8th degree (12km) resolution. Surface variables such as solar radiation and surface temperatures are available hourly, while upper level atmospheric variables such as wind and pressure are available 3-hourly. All 3 hourly variables were linearly interpolated to hourly. Upper-level atmospheric data that is only available at specific pressure levels was interpolated to the appropriate turbine hub heights of each wind power plant.

Downward shortwave solar radiation, also known as Global Horizontal Irradiance (GHI), is an available variable from TGW. Diffuse solar radiation was produced using the simulated GHI and the DISC model [40, 41]. DISC has known biases when used under clear sky conditions so bias correction was applied to the final solar generation data.

One potential challenge in utilizing the TGW data is the uncertainty around the capability of the 1/8th degree TGW data to accurately capture cloud radiative effects – the impact of clouds on the amount of longwave (LW) and shortwave (SW) radiation that reaches the surface. At this resolution the majority of clouds, and thus their resulting impacts on surface radiation, must be parameterized in the model that produced the TGW data. The paramaterization of cloud radiative effects is scale dependent [42]. Furthermore, the strongest shortwave cloud radiative effects come from shallow cumulus clouds which are not resolved at this scale (e.g., [43]). Collectively this means that the surface SW and LW radiation in the TGW data may be biased. To account for the biases in the solar radiation data, National Solar Radiation Database (NSRDB) data was collected at every plant location and run through identical solar generation models [44]. Bias correction was then applied to the generation data [34]. Bias correction typically lowered the solar generation by approximately 10%.

Using the TGW meteorology data, hourly wind and solar generation profiles were produced across the CONUS for every wind and solar plant that is listed in the EIA-860 2020 database [35]. Power plant configurations were developed using EIA-860 data. These plant configurations along with the TGW meteorological data were used as inputs to the NREL reV model [45, 46] to produce hourly generation data for each plant.

2.2. Load Data

To characterize energy supply droughts we produced historical hourly total load projections that correspond temporally and spatially to the wind and solar generation data. Loads were produced using the Total ELectricity Loads (TELL) model which downscales simulated annual state-level electricity demands to an hourly resolution [47, 48]. The input data to TELL is hourly time series of meteorology from the same TGW dataset that underpins the wind and solar generation simulations. TELL then uses the hour-to-hour variations in weather to model total load for each BA. Because they are based on the same hourly gridded meteorology forcing the load, the simulations from TELL and the wind and solar generation simulations are temporally and spatially coincident.

Over the 40 year historical period of the data, load has had an upward trend due to rising population and, more recently, electrification. To account for such an upward trend, each year of data was normalized by subtracting the annual mean and dividing by the annual standard deviation for each Balancing Authority (BA). BAs are North American energy regions that are required to balance total generation with load locally before relying on neighboring interconnected regions. There are 69 BAs across the U.S. (as of 2020) which are equivalent to countries or sub regions in other continental bulk power grids. The per-year per-BA load normalization allows for every year's load to be analyzed equally and consistently using a percentile based threshold, described in the next Section 3.

2.3. Hourly BA-level Generation Data

Plant-level wind and solar generation data were aggregated by BA. Due to the intermittency of the resources, hourly wind and solar datasets are typically described either in MWh or with capacity factors. In this study, generation is expressed as a capacity factor which is total generation divided by total plant capacity. Only those BAs that had a minimum of 5 wind and solar plants were included so that the results are not unduly influenced by a single plant. This resulted in 15 BAs for this analysis that span the CONUS (Figure 1). The BAs cover most of the CONUS except for the southeast region due to lack of wind plants. The 2020 fleet includes 2,817 solar plants and 1,151 wind plants (Table 1). The final dataset used in the analysis thus consists of hourly wind and solar generation and coincident total load for each BA from 1980-2019 (40 years) for 15 BAs.

3. Methodology

Energy droughts have multiple definitions in the literature, but generally the goal is the same in every definition: to define a period of time during which variable energy generation is low. The definition is dependent on the threshold that is used to flag a low period as well as the resolution of the input data. Definitions in the literature tend to look at daily data, but given that we have hourly data it is possible to look at a variety of time scales from sub-daily to multi-day. This range of resolutions aims to address specific temporal scales in bulk power grid operations, specifically to address the need and optimal dispatch of sub-daily storage and management of longer duration storage. Energy production droughts are those which only involve low energy production, in this case wind and solar. A production drought might not have any grid impacts if load is low. Energy supply droughts incorporate energy demand into the definition and quantify drought severity in terms of demand or load shortfall.

3.1. Energy Droughts - Sub-Daily to Multi-Day

To define energy droughts we adopt the indices introduced by [32]. Standardized indices offer a consistent scale that enables the comparison of droughts both within a single study and across

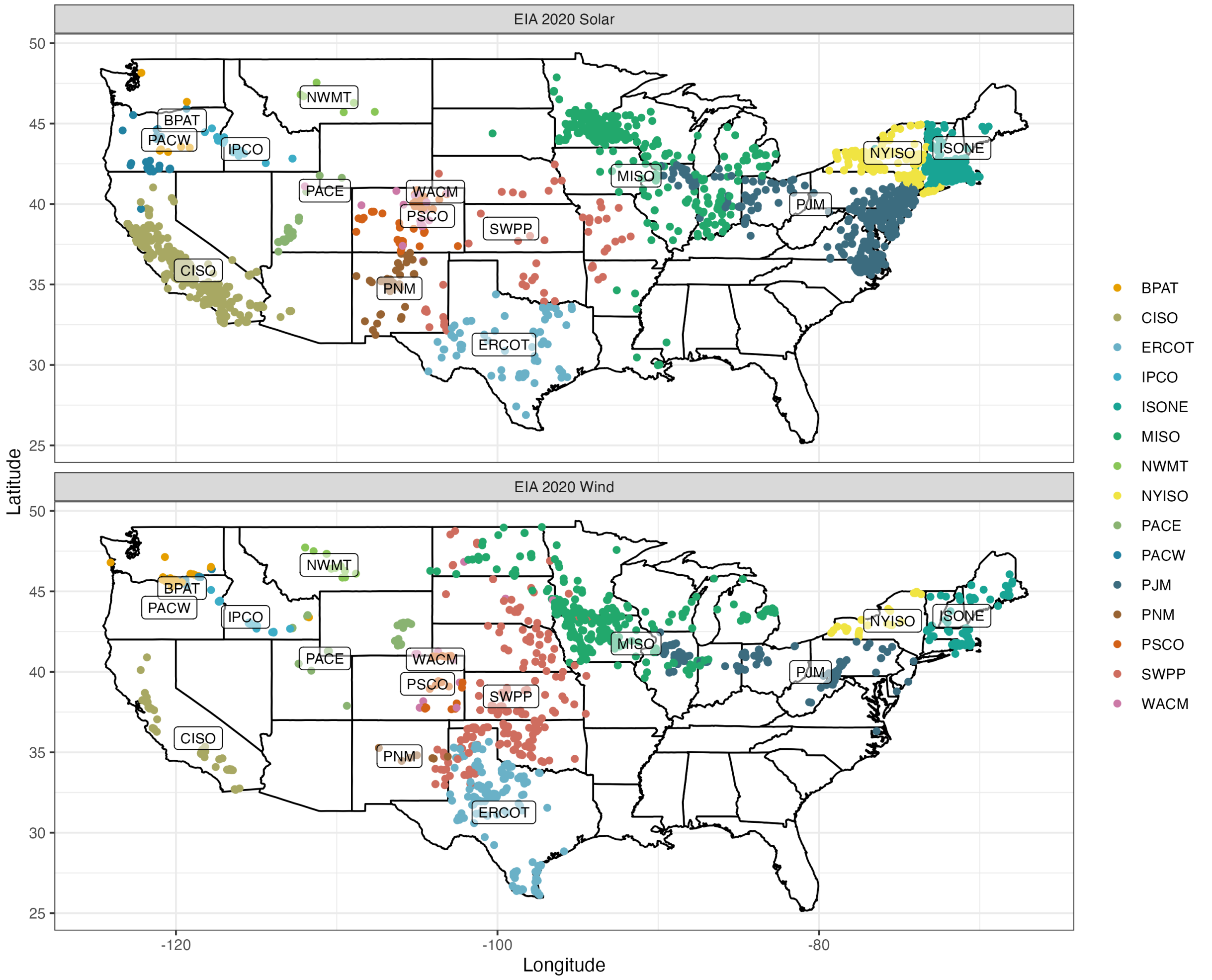

Figure 1: Wind and solar plant locations for each BA in the CONUS that contains at least 5 wind and solar plants.

multiple studies, and bring the definition of energy droughts in line with other fields such as hydrology and climatology. For wind and solar, the index introduced by [32] is called the standardized renewable energy production index (SREPI)

$$\mathrm{SREPI}(P_t) = \Phi^{-1}\left(\frac{1}{n+2}\left[1 + \sum_{i=1}^{n} \mathbb{1}\{P_i \leq P_t\}\right]\right)$$

where P_t represents the solar or wind production at time t, Φ^{-1} is the standard normal quantile function, n is the number of points in a particular period of interest, $\mathbb{1}$ is the indicator function which returns 1 if the bracketed expression is true, 0 otherwise. The $n+2$ and $1+$ terms are plotting position adjustments so that the empirical cumulative distribution will never equal 0 or

BA Code	BA Name	Solar Plant Count	Wind Plant Count	Solar Capacity (MW)	Wind Capacity (MW)
BPAT	Bonneville Power Administration	11	29	88	3398
CISO	California Independent System Operator	572	125	14789	5836
ERCOT	Electric Reliability Council of Texas, Inc.	76	163	4864	27753
IPCO	Idaho Power Company	20	33	318	717
ISNE	ISO New England Inc.	518	82	1528	1504
MISO	Midcontinent Independent Transmission System Operator, Inc.	545	401	2056	26101
NWMT	NorthWestern Energy	6	16	17	453
NYISO	New York Independent System Operator	226	33	664	1989
PACE	PacifiCorp - East	34	30	1286	2690
PACW	PacifiCorp - West	29	19	294	694
PJM	PJM Interconnection, LLC	644	129	4557	10159
PNM	Public Service Company of New Mexico	51	7	370	1066
PSCO	Public Service Company of Colorado	68	28	519	4491
SWPP	Southwest Power Pool	55	224	393	24267
WACM	Western Area Power Administration Rocky Mountain Region	26	17	192	782

Table 1: Balancing Authorities used in this study along with the number of wind and solar plants per BA and the installed capacity of wind and solar as of 2020.

1, for which cases the indices are not well defined [32].

For load, the index is known as the standardized residual load index (SRLI)

$$\mathrm{SRLI}(P_t) = \Phi^{-1}\left(\frac{1}{n+2}\left[1 + \sum_{i=1}^{n} \mathbb{1}\{L_i \leq L_t\}\right]\right)$$

where L_t represents the residual load at time t. We define residual load in this study as load minus wind and solar production. In the analysis residual load is expressed as a fraction of the maximum residual load in the period so that the load data is on the same scale as the wind and solar capacity factors.

It is necessary when applying these indices to select a period of interest, which is used to construct the empirical distribution functions and compute the indices. We elect to define the distributions across all years of data, by week of the year, and by hour of the day in the case of sub-daily droughts. This approach has the benefit of revealing abnormal sub-daily to sub-seasonally drought conditions in all seasons, instead of only occurring where both wind and solar are seasonally low and addressing the need for other types of multi-season storage technologies or thermo-electric plants like nuclear technologies for base load.

With the indices for load, wind and solar computed we turn to the definitions of energy droughts. In this study, we define two types of droughts - production and supply: Wind and Solar (WS) and Load, Wind, and Solar (LWS) respectively. We presently have not included hydropower as the time scales involved are much longer and can be addressed with cross-seasonal water management in future studies. WS droughts occur when both wind and solar SREPI values fall below -1.28 for the entire drought period, which corresponds to the 10th percentile or below of production in both resources. The drought may last 2 hours or more[1]. LWS droughts use the same definition for wind and solar but add in a third criteria where the SRLI must also fall above 1.28 for the entire drought period (which corresponds to a 90th percentile threshold for load). According to the thresholds in [32], this would be classified as a Moderate drought. Drought definitions are summarized in Table 2. Sensitivity analysis for the 10th percentile threshold is presented in the supplemental materials (Figure A.7 and Figure A.8).

Drought type	Drought definition
Wind and Solar (WS)	SREPI(W_t) < -1.28 and SREPI(S_t) < -1.28
Load, Wind and Solar (LWS)	SRLI(L_t) > 1.28 and SREPI(W_t) < -1.28 and SREPI(S_t) < -1.28

Table 2: Definitions for WS and LWS droughts. SREPI(W_t), SREPI(S_t) and SRLI(L_t) indicate the wind, solar and load index values at time t, respectively.

We compute energy droughts for seven time scales: 1-hour, 4-hour, 12-hour, 1-day, 2-day, 3-day, and 5-day. When utilizing time scales of greater than one hour (4-hour or more), the energy is totaled over the period and the threshold is applied to the aggregated data. This allows for the possibility that not every hour during a drought period falls below the threshold. For time scales of less than one day (1-, 4- and 12-hour), one should keep in mind that the nighttime period has no solar generation. We allowed the nighttime period for solar to function as a wild card, i.e. droughts

[1]We excluded droughts lasting only 1 hour due to excessive noise in the data, all other time scales the droughts can last 1 timestep or longer

that start before the nighttime where the wind is still below the threshold, are allowed to continue overnight.

3.2. Drought Frequency, Duration and Magnitude

In order to identify potential grid impacts and to inform grid planning, specific information about drought frequency, duration, and magnitude are necessary. Frequency is defined as the average number of droughts in a year across the 40 year historical record. Duration is defined by the number of consecutive timesteps falling below (or above in the case of load) the percentile threshold, multiplied by the timestep length.

Drought magnitude for a single variable is defined by the summation of the absolute value of the index (SREPI or SRLI) over the drought period [32]. This definition works well for single variable droughts when using a single time scale, but is not suitable to compare droughts across different time scales and between different compound drought events (WS vs. LWS). For example, shorter time scales will tend to have higher drought magnitude simply due to having more timesteps. In addition, compound droughts with more variables will appear to have a larger magnitude due to more variables being added up each timestep. For these reasons, we found it necessary to modify the definition of drought magnitude slightly. For compound droughts we define the magnitude to be the sum of average of the absolute values of the indices involved in the drought, effectively providing a single average drought magnitude that is on the same scale as the original indices. Given n variables each corresponding to a standardized index in $I_1, ..., I_n$, respectively, the compound drought magnitude (CDM) is defined as

$$\text{CDM} = \frac{1}{nD} \sum_{j=t}^{t+D-1} \sum_{k=1}^{n} |I_k|$$

where CDM is the compound drought magnitude, t is the first timestep of the drought, D is the drought duration. For example, for a LWS drought,

$$\text{CDM}_{\text{LWS}} = \frac{1}{3D} \left[\sum_{j=t}^{t+D-1} |\text{SREPI}(W_j)| + |\text{SREPI}(S_j)| + |\text{SRLI}(L_j)| \right]$$

For WS droughts this can be easily modified by excluding the SRLI term and dividing by 2 instead of 3.

4. Results

4.1. Duration

WS drought duration is of particular interest for grid resource planning and storage sizing. Figure 2 shows empirical cumulative distribution functions (CDFs) of drought duration of the entire historical record for 3 time scales. 1-hour droughts are those in which every subsequent hour consistently measures below the 10th percentile threshold; This is useful for applications to sub-daily unit commitment. 1-day droughts are those with consecutive days in which the total energy falls below the threshold for each successive day; they are intended for applications to day ahead market and unit commitment. 3-day droughts are determined similarly to 1-day droughts and are intended for managing longer term storage and daily resources with limited ability to recharge daily. We note that all the BAs show remarkable similarity in the duration of droughts across all time scales as shown by similar CDF shapes. 1-hour WS droughts in the CONUS never last more than about 1.5 days, with the longest drought of about 37 hours occurring in Texas (ERCOT). The shortest 1-hour maximum duration across BAs is roughly 16 hours in California (CISO). The 1-hour drought duration across the CONUS is strongly driven by the solar variability which is in turn driven by cloud variability – droughts based solely on wind exhibit much longer durations (not shown). For 1-day and 3-day time scales, California (CISO) exhibits the longest duration of WS droughts at 6 days and 9 days, respectively. BPAT in the Pacific Northwest has the shortest maximum duration at about 2 days and 3 days, respectively. In general, CISO stands out as the BA with the longest duration of droughts at 1-day time scales or longer and ERCOT tends to have the longest droughts at shorter time scales.

4.2. Compound Drought Magnitude

In the methodology section we introduced the CDM metric with the ability to compare droughts across time scales and when using different number of variables such as WS (production) vs. LWS (supply) droughts. Figure 3 shows the CDM for all BAs across all time scales. All BAs are grouped together for a particular time scale to show the utility of the CDM metric. Clearly LWS droughts are higher in magnitude than WS droughts across all time scales. This finding is significant and indicates that on average wind and solar droughts that co-occur with high loads are more severe than those that occur otherwise. This may be due to WS droughts occurring more often during

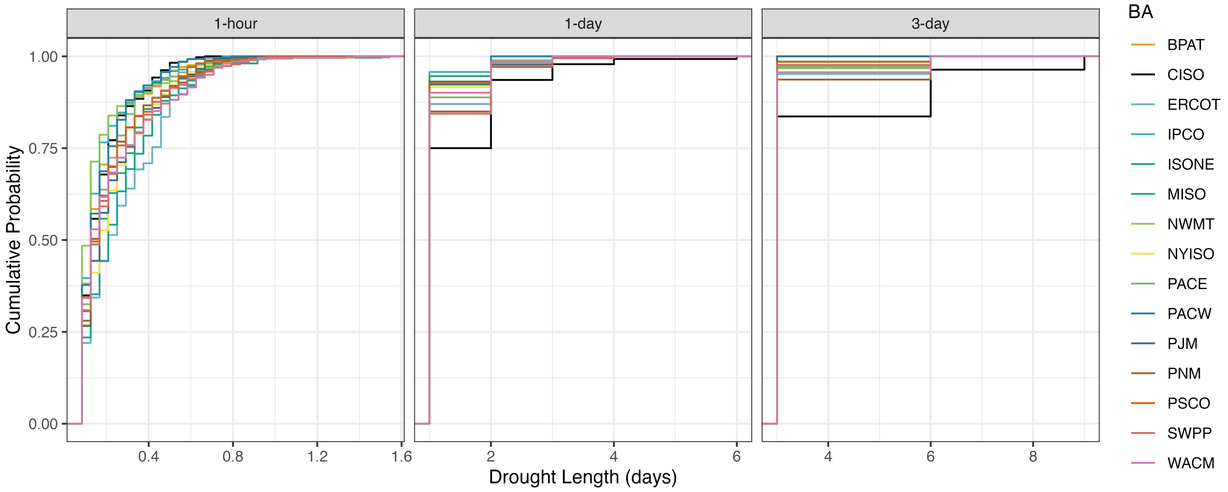

Figure 2: Empirical CDFs for WS drought duration, for 1-hour, 1-day and 3-day time scales. CISO is highlighted in black as it tends to be the BA with the longest duration droughts at time scales longer than hourly.

extreme temperature conditions when load is high. More research is necessary to determine the specific meteorological mechanisms, but this statistical finding may be of interest to grid planners. Also of note, there is a minor decrease in the magnitude of both LWS and WS droughts as time scale increases. At longer time scales the criteria for droughts is harder to satisfy so those droughts that do meet the criteria tend to be less severe.

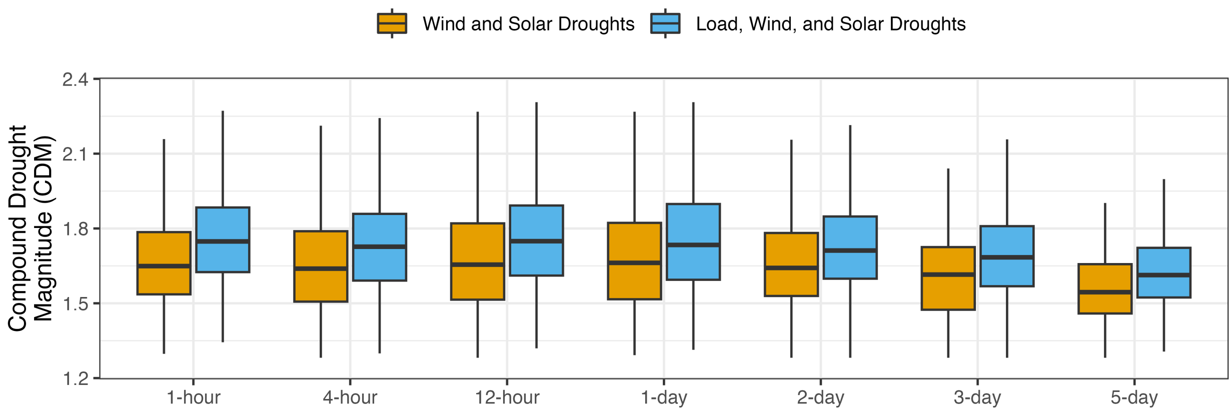

Figure 3: CDM for WS and LWS droughts for all BAs across all time scales.

4.3. Spatial distribution of frequency and maximum duration

Figure 4 shows the frequency and maximum duration of droughts in all the BAs included in the study for a 1-hour and 1-day time scale. The size of the dots indicates the number of events per year and the color indicates the maximum drought duration observed during the historical period. 1-hour droughts exhibit some spatial grouping in terms of drought duration, such as the Rocky Mountains, and across the north. Daily droughts also show a clear spatial pattern. Duration tends to be shorter (0-2 days) in the northern BAs and longer in the southern BAs (2-4 days), with CISO again standing out as having the longest duration droughts (4-6 days). The most frequent 1-hour droughts (9-13 per year) occur in the central and Rocky Mountain regions, while the least frequent droughts occur in the northern regions (5-9 per year). A similar spatial pattern is present in the 1-day droughts with the most frequent events (4-6 per year) occurring in the central and Rocky Mountain regions and the least frequent events (2-4 per year) occurring in the northern regions. This result is somewhat counter-intuitive as one might expect that regions with less solar production, simply due to higher latitude or climatological conditions, might have more frequent droughts. In this study, energy droughts are only identified when solar and wind production is abnormally low for a particular period of the year, effectively excluding seasonal signals. In regions where low solar production is typical, it is more difficult to have abnormally low conditions compared to regions where high production is normal, and thus there are less frequent sub-seasonal droughts.

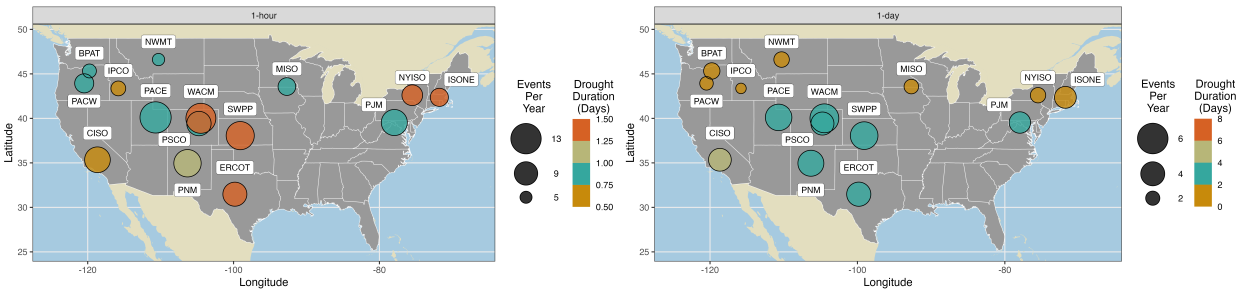

Figure 4: Hourly (left panel) and daily (right panel) droughts. The maximum drought duration is indicated by the bubble color and the the drought frequency is indicated by the size of the bubble. Note the scale of the drought frequency is different in each panel.

4.4. Seasonal Distribution of Droughts

Figure 5 shows the seasonal distributions of daily energy droughts for each BA. Most BAs do not exhibit a strong seasonal drought signal, except for CISO where droughts are far more common in the summer months. Drought duration also does not exhibit a strong seasonal distribution. These results indicate that in most BAs across the CONUS (except CISO), compound WS droughts have an approximately equal probability of occurring in any season. It is worth noting that the lack of seasonal signal in most BAs is expected and certainly related to the way droughts are defined in this study. We chose to use a moving threshold that changes based on the week of the year. If droughts were defined based on a single yearly threshold, then they would occur most often at the time of the year when the wind and solar were both climotologically lowest and would impact different storage technologies (seasonal). When defined using a fixed threshold droughts tend to occur more often and with longer duration in the fall and winter though the timing does vary substantially between BAs (Figure A.9).

4.5. WS vs. LWS Droughts

In order to summarise the average behavior of WS and LWS droughts, Figure 6 displays average frequency (events per year) and duration of droughts in days for all 15 BAs. The left panel shows WS droughts and the right panel shows LWS droughts. About half as many LWS droughts tend to occur each year compared to WS. While a decrease in frequency is expected due to the extra load criteria placed on the drought definition, this reduction in frequency is smaller than expected if high load events were independent of WS droughts. Given the 90th percentile threshold used in the definition of LWS droughts, we would expect the frequency of LWS droughts to drop by 90% if the WS droughts were equally distributed across all potential load values. The fact that the frequency of events instead only drops by 50% suggests that the WS droughts preferentially occur during periods of high loads.

In Figure 6, 1-hour and 4-hour time scale droughts have nearly indistinguishable average durations, while other time scales tend to cluster just above the minimum duration possible. The vertical lines from each point span from the minimum drought duration to the maximum, indicating that the drought duration distributions are highly skewed. The durations do not exhibit significant differences between WS droughts and LWS droughts.

Figure 5: Seasonal distributions of energy droughts. The bar heights indicate the frequency of droughts in a particular month (average number of droughts per year). The color indicates the drought duration.

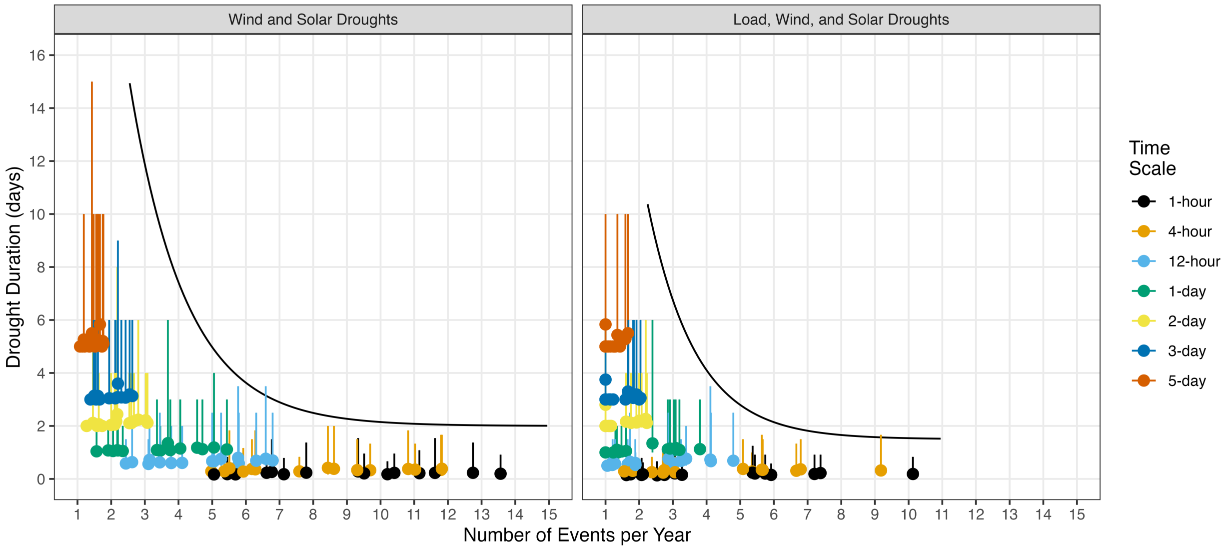

Figure 6: Magnitude, duration and frequency of energy droughts for all BAs and aggregation periods. WS droughts are shown in the left panel and LWS droughts in the right panel. The points indicate the mean drought duration for a BA at a given time scale, the vertical lines indicate the range of drought durations from the min to the max observed duration in the 40 year period. The curved line is an exponential curve meant to illustrate a rough upper bounding region for the data.

5. Limitations and Discussion

In this section we discuss some of the limitations of this study and broader implications. First and foremost, hydropower is not represented in this study. In some regions, like the Pacific Northwest, hydropower is a dominant source of renewable energy such that integrating wind and solar and mitigating local energy droughts to 6 days is not a major concern. In other regions, hydropower is a conserved resource critical for ramping, energy storage, and mitigating the cost of additional battery storage to manage wind and solar droughts. In this study we focus on sub-daily to multi-day droughts without consideration of hydropower since water resources at those scales can most often be managed to mitigate those droughts if the market incentives are present. For studies which consider seasonal or longer period droughts, hydropower should be considered.

Drought studies at the BA scale are strategic to understand the potential need for local storage, and innovate on commitment approaches and market incentives. Even though we looked into LWS (supply) droughts, we note that adjacent BAs linked by transmission may display seasonal complementarities and thus reduce the local stress. This research needs to feed into more complete studies where production cost models are involved in evaluating local storage versus transmission with social equity impacts. Those production cost model simulations are resources intensive and our approach identifies events to prioritize.

We chose to use a 10th percentile benchmark in this study across wind, solar and load. Although we do provide a sensitivity analysis in the appendix, such thresholds alone may not represent conditions that are extreme enough to stress the grid, even when compound events are considered. Our study could be complemented with thermal derating and forced power outages when reaching certain thresholds which would accentuate the impact of droughts. In that sense, 10 percent is a regional standardized threshold but derating and unit outages could add a different dimension to the overall severity. Finally, the choice to use a fixed or moving threshold has implications that vary by application and by region – a more detailed exploratory analysis should likely consider both approaches. Nonetheless this work represents the first benchmark of standardized contemporary energy production and supply droughts by BA over the CONUS.

6. Conclusions

In this study we present a methodology and dataset for examining compound wind and solar energy droughts that have the potential to impact the power grid dynamics and local supply. Specifically we provide the first standardized benchmark of energy droughts in the Continental United States (CONUS). By focusing our results on 15 Balancing Authorities (BAs) with numerous utility scale wind and solar plants, we are able to draw conclusions that are applicable to grid planning and storage sizing. BA-level load was included to quantify high residual load coincident with Wind and Solar (WS) droughts, providing a view of the potential impact of compound Load, Wind, and Solar (LWS) events. We utilized a dataset of hourly BA level generation which includes thousands of 2020 infrastructure wind and solar plants. Using this dataset we examine the frequency, duration, and magnitude of energy droughts at a variety of temporal and spatial scales.

To classify compound droughts we utilize the standardized renewable energy production index (SREPI) and the standardized residual load index (SRLI). This study is the first application of these indices outside of the original paper focusing on the development of the indices and a case study in Europe [32]. In addition, we introduce a definition of compound drought magnitude (CDM) that is suitable for comparing droughts across different timescales and with any number of variables.

WS droughts are typically less frequent and shorter in the northern CONUS compared to other regions. California stands out as having the longest duration droughts at time scales 1-day or longer but having among the shortest duration of droughts at shorter time scales. Droughts in California also show a strong seasonality, tending to occur in the summer, while other BAs tend to show a more even distribution across the year. Adjacent droughts in the Pacific Northwest and Rockies tend to have some of the lowest and highest drought frequencies, respectively. At shorter timescales, eastern BAs have some of the longest drought durations recorded. Existing hydropower resources in the area may be able to mitigate this given the drought durations tend to be low to moderate at longer time scales. ERCOT which covers most of Texas, has limited interconnections with other BAs. It also has some of the longest 1-hour droughts in the record, although at longer timescales the droughts are on the lower end compared to other BAs. This suggests a need for short term storage infrastructure in a decarbonized future.

LWS droughts differ from WS droughts notably in the average frequency of events per year, suggesting that WS droughts occur preferentially with high load events. Additionally, LWS droughts exhibit higher magnitudes on average than WS droughts. Both of these findings have implications to grid planning and storage sizing. WS and LWS droughts exhibit similar durations across all time scales.

The standardized approach in this study supports the synthesis of this type of research at storage and energy system security scales. This research on standardized drought informs research in storage, transmission siting and sizing, characterization of extreme events for climate stress tests and reliability studies. Some potential future work includes i) incorporating derating and forced outages, ii) applications to evolving infrastructure, iii) future climate, and v) future markets since a "must-take" approach in the U.S. may not be appropriate under deep decarbonization scenarios.

7. Data and Code Availability

The energy drought analytics and dataset developed in this paper is available at:

`https://zenodo.org/record/8008034`

The code used to conduct the analysis and produce the figures is available on GitHub:

`https://github.com/GODEEEP/energy-droughts`

8. Credit Author Statement

Cameron Bracken: Conceptualization, Data curation, Formal analysis, Investigation, Methodology, Software, Visualization, Roles/Writing – original draft. Nathalie Voisin: Conceptualization, Methodology, Supervision, Writing – review & editing. Casey Burleyson: Data curation, Writing – review & editing. Allison Campbell: Conceptualization, Writing – review & editing. Z. Jason Hou: Conceptualization, Writing – review & editing. Daniel Broman: Conceptualization.

9. Funding

This research was supported by the Grid Operations, Decarbonization, Environmental and Energy Equity Platform (GODEEEP) Investment, under the Laboratory Directed Research and Development (LDRD) Program at Pacific Northwest National Laboratory (PNNL).

PNNL is a multi-program national laboratory operated for the U.S. Department of Energy (DOE) by Battelle Memorial Institute under Contract No. DE-AC05-76RL01830.

References

[1] K. van der Wiel, L. P. Stoop, B. R. H. van Zuijlen, R. Blackport, M. A. van den Broek, F. M. Selten, Meteorological conditions leading to extreme low variable renewable energy production and extreme high energy shortfall, Renewable and Sustainable Energy Reviews 111 (2019) 261–275. doi:10.1016/j.rser.2019.04.065.

[2] D. Raynaud, B. Hingray, B. François, J. D. Creutin, Energy droughts from variable renewable energy sources in european climates, Renewable Energy 125 (2018) 578–589. doi:10.1016/j.renene.2018.02.130.

[3] D. Rife, N. Y. Krakauer, D. S. Cohan, J. C. Collier, A new kind of drought: Us record low windiness in 2015, Earthzine (2016).
URL https://earthzine.org/a-new-kind-of-drought-u-s-record-low-windiness-in-2015/

[4] B. Shen, F. Kahrl, A. J. Satchwell, Facilitating power grid decarbonization with distributed energy resources: Lessons from the united states, Annual Review of Environment and Resources 46 (1) (2021) 349–375. doi:10.1146/annurev-environ-111320-071618.

[5] A. Dyreson, N. Devineni, S. W. D. Turner, T. D. S. M, A. Miara, N. Voisin, S. Cohen, J. Macknick, The role of regional connections in planning for future power system operations under climate extremes, Earth's Future 10 (6) (jun 2022). doi:https://doi.org/10.1029/2021EF002554.

[6] K. Doering, C. L. Anderson, S. Steinschneider, Evaluating the intensity, duration and frequency of flexible energy resources needed in a zero-emission, hydropower reliant power system, Oxford Open Energy 2 (2023). doi:https://doi.org/10.1093/ooenergy/oiad003.

[7] N. Otero, O. Martius, S. Allen, H. Bloomfield, B. Schaefli, Characterizing renewable energy compound events across europe using a logistic regression-based approach, Meteorological Applications 29 (5) (2022) e2089. doi:10.1002/met.2089.

[8] J. A. Ferraz de Andrade Santos, P. de Jong, C. Alves da Costa, E. A. Torres, Combining wind and solar energy sources: Potential for hybrid power generation in brazil, Utilities Policy 67 (2020) 101084. doi:10.1016/j.jup.2020.101084.

[9] J. Jurasz, J. Mikulik, P. B. Dabek, M. Guezgouz, B. Kaźmierczak, Complementarity and 'resource droughts' of solar and wind energy in poland: An era5-based analysis, Energies 14 (4) (2021) 1118. doi:10.3390/en14041118.

[10] N. Otero, O. Martius, S. Allen, H. Bloomfield, B. Schaefli, A copula-based assessment of renewable energy droughts across europe, Renewable Energy 201 (2022) 667–677. doi:10.1016/j.renene.2022.10.091.

[11] B. François, M. Borga, J. Creutin, B. Hingray, D. Raynaud, J. Sauterleute, Complementarity between solar and hydro power: Sensitivity study to climate characteristics in northern-italy, Renewable Energy 86 (2016) 543–553. doi:10.1016/j.renene.2015.08.044.

[12] P. T. Brown, D. J. Farnham, K. Caldeira, Meteorology and climatology of historical weekly wind and solar power resource droughts over western north america in ERA5, SN Applied Sciences 3 (10) (sep 2021). doi:10.1007/s42452-021-04794-z.

[13] B. Li, S. Basu, S. J. Watson, H. W. J. Russchenberg, A brief climatology of dunkelflaute events over and surrounding the north and baltic sea areas, Energies 14 (20) (2021) 6508. doi:https://doi.org/10.3390/en14206508.

[14] D. Tong, D. J. Farnham, L. Duan, Q. Zhang, N. S. Lewis, K. Caldeira, S. J. Davis, Geophysical constraints on the reliability of solar and wind power worldwide, Nature Communications 12 (1) (2021) 6146. doi:10.1038/s41467-021-26355-z.

[15] K. Engeland, M. Borga, J.-D. Creutin, B. François, M.-H. Ramos, J.-P. Vidal, Space-time variability of climate variables and intermittent renewable electricity production – a review, Renewable and Sustainable Energy Reviews 79 (2017) 600–617. doi:10.1016/j.rser.2017.05.046.

[16] K. Mohammadi, N. Goudarzi, Study of inter-correlations of solar radiation, wind speed and precipitation under the influence of el niño southern oscillation (enso) in california, Renewable Energy 120 (2018) 190–200. doi:10.1016/j.renene.2017.12.069.

[17] L. Lledó, O. Bellprat, F. J. Doblas-Reyes, A. Soret, Investigating the effects of pacific sea surface temperatures on the wind drought of 2015 over the united states, Journal of Geophysical Research: Atmospheres 123 (10) (2018) 4837–4849. doi:https://doi.org/10.1029/2017JD028019.

[18] J. Jurasz, A. Beluco, F. A. Canales, The impact of complementarity on power supply reliability of small scale hybrid energy systems, Energy 161 (2018) 737–743. doi:10.1016/j.energy.2018.07.182.

[19] A. Solomon, D. M. Kammen, D. Callaway, Investigating the impact of wind–solar complementarities on energy storage requirement and the corresponding supply reliability criteria, Applied Energy 168 (2016) 130–145. doi:10.1016/j.apenergy.2016.01.070.

[20] S. Potrč, A. Nemet, L. Čuček, P. S. Varbanov, Z. Kravanja, Synthesis of a regenerative energy system – beyond carbon emissions neutrality, Renewable and Sustainable Energy Reviews 169 (2022) 112924. doi:

10.1016/j.rser.2022.112924.

[21] V. Gburčik, S. Mastilović, Željko Vučinić, Assessment of solar and wind energy resources in serbia, Journal of Renewable and Sustainable Energy 5 (4) (2013) 041822. doi:10.1063/1.4819504.

[22] H. C. Bloomfield, D. J. Brayshaw, A. J. Charlton-Perez, Characterizing the winter meteorological drivers of the european electricity system using targeted circulation types, Meteorological Applications 27 (1) (2020) e1858. doi:10.1002/met.1858.

[23] P. E. Bett, H. E. Thornton, The climatological relationships between wind and solar energy supply in britain, Renewable Energy 87 (2016) 96–110. doi:10.1016/j.renene.2015.10.006.

[24] B. François, B. Hingray, D. Raynaud, M. Borga, J. D. Creutin, Increasing climate-related-energy penetration by integrating run-of-the river hydropower to wind/solar mix, Renewable Energy 87 (2016) 686–696. doi:10.1016/j.renene.2015.10.064.

[25] M. M. Miglietta, T. Huld, F. Monforti-Ferrario, Local complementarity of wind and solar energy resources over europe: An assessment study from a meteorological perspective, Journal of Applied Meteorology and Climatology 56 (1) (2017) 217–234. doi:10.1175/jamc-d-16-0031.1.

[26] H. C. Bloomfield, C. C. Suitters, D. R. Drew, Meteorological drivers of european power system stress, Journal of Renewable Energy 2020 (2020) 5481010. doi:10.1155/2020/5481010.

[27] M. Gonzalez-Salazar, W. Roger Poganietz, Making use of the complementarity of hydropower and variable renewable energy in latin america: A probabilistic analysis, Energy Strategy Reviews 44 (2022) 100972. doi:10.1016/j.esr.2022.100972.

[28] H. C. Bloomfield, C. M. Wainwright, N. Mitchell, Characterizing the variability and meteorological drivers of wind power and solar power generation over africa, Meteorological Applications 29 (5) (2022) e2093. doi:10.1002/met.2093.

[29] K. Doering, S. Steinschneider, Summer covariability of surface climate for renewable energy across the contiguous united states: Role of the north atlantic subtropical high, Journal of Applied Meteorology and Climatology 57 (12) (2018) 2749–2768. doi:10.1175/jamc-d-18-0088.1.

[30] K. Z. Rinaldi, J. A. Dowling, T. H. Ruggles, K. Caldeira, N. S. Lewis, Wind and solar resource droughts in california highlight the benefits of long-term storage and integration with the western interconnect, Environmental Science & Technology 55 (9) (2021) 6214–6226. doi:10.1021/acs.est.0c07848.

[31] Y. Amonkar, D. J. Farnham, U. Lall, A k-nearest neighbor space-time simulator with applications to large-scale wind and solar power modeling, Patterns 3 (3) (2022) 100454. doi:10.1016/j.patter.2022.100454.

[32] S. Allen, N. O. Felipe, Standardised indices to monitor energy droughts, SSRN Electronic Journal (2022). doi:10.2139/ssrn.4312835.

[33] T. B. McKee, N. J. Doesken, J. Kleist, The relationship of drought frequency and duration to time scales, Eighth Conference on Applied Climatology (1993).

[34] A. Campbell, C. Bracken, S. Underwood, N. Voisin, Dynamically downscaled power production for all eia wind and solar power plants, submitted (2023).

[35] Form EIA-860 detailed data with previous form data (EIA-860A/860B) (2023).
URL https://www.eia.gov/electricity/gridmonitor/about

[36] C. Bracken, S. Underwood, A. Campbell, T. B. Thurber, N. Voisin, Hourly wind and solar generation profiles for every EIA 2020 plant in the CONUS (May 2023). doi:10.5281/zenodo.7901615.

[37] A. D. Jones, D. Rastogi, P. Vahmani, A. Stansfield, K. Reed, T. Thurber, P. Ullrich, J. S. Rice, Im3/hyperfacets thermodynamic global warming (tgw) simulation datasets (v1.0.0) (2022). doi:10.57931/1885756.

[38] A. Jones, D. Rastogi, P. Vahmani, A. Stansfield, K. Reed, T. Thurber, P. Ullrich, J. Rice, Continental united states climate projections based on thermodynamic modification of historical weather, submitted (2023).

[39] H. Hersbach, B. Bell, P. Berrisford, G. Biavati, A. Horányi, J. Muñoz Sabater, J. Nicolas, C. Peubey, R. Radu, I. Rozum, D. Schepers, A. Simmons, C. Soci, D. Dee, J.-N. Thépaut, Era5 hourly data on single levels from 1940 to present, Copernicus Climate Change Service (C3S) Climate Data Store (CDS) (2023). doi:10.24381/cds.adbb2d47.

[40] E. Maxwell, A quasi-physical model for converting hourly global horizontal to direct normal insolation, techreport, NREL (1987).

[41] A. Skartveit, J. A. Olseth, M. E. Tuft, An hourly diffuse fraction model with correction for variability and surface albedo, Solar Energy 63 (3) (1998) 173–183. doi:10.1016/S0038-092X(98)00067-X.

[42] F. Senf, A. Voigt, N. Clerbaux, A. Hünerbein, H. Deneke, Increasing resolution and resolving convection improve the simulation of cloud-radiative effects over the north atlantic, Journal of Geophysical Research: Atmospheres 125 (19) (oct 2020). doi:10.1029/2020JD032667.

[43] C. D. Burleyson, C. N. Long, J. M. Comstock, Quantifying diurnal cloud radiative effects by cloud type in the tropical western pacific, Journal of Applied Meteorology and Climatology 54 (6) (2015) 1297–1312. doi:10.1175/JAMC-D-14-0288.1.

[44] M. Sengupta, Y. Xie, A. Lopez, A. Habte, G. Maclaurin, J. Shelby, The national solar radiation data base (NSRDB), Renewable and Sustainable Energy Reviews 89 (2018) 51–60. doi:https://doi.org/10.1016/j.rser.2018.03.003.

[45] G. Maclaurin, N. Grue, A. Lopez, D. Heimiller, M. Rossol, G. Buster, T. Williams, The renewable energy potential (reV) model: A geospatial platform for technical potential and supply curve modeling (sep 2019). doi:https://doi.org/10.2172/1563140.

[46] G. Buster, M. Rossol, P. Pinchuk, R. Spencer, B. N. Benton, M. Bannister, T. Williams, The renewable energy potential model (rev) (Feb. 2023). doi:10.5281/zenodo.7641483.
URL https://doi.org/10.5281/zenodo.7641483

[47] C. R. McGrath, C. D. Burleyson, Z. Khan, A. Rahman, T. Thurber, C. R. Vernon, N. Voisin, J. S. Rice, tell: a python package to model future total electricity loads in the united states (nov 2022). doi:10.21105/joss.04472.

[48] Hourly Electric Grid Monitor (2023).
URL https://www.eia.gov/electricity/gridmonitor/about

Appendix A. Supplemental Material

Figure A.7 shows a sensitivity analysis of drought duration by changing the percentile threshold for the 1-day time scale. The dashed lines show the min and max duration and the solid line is the average duration.

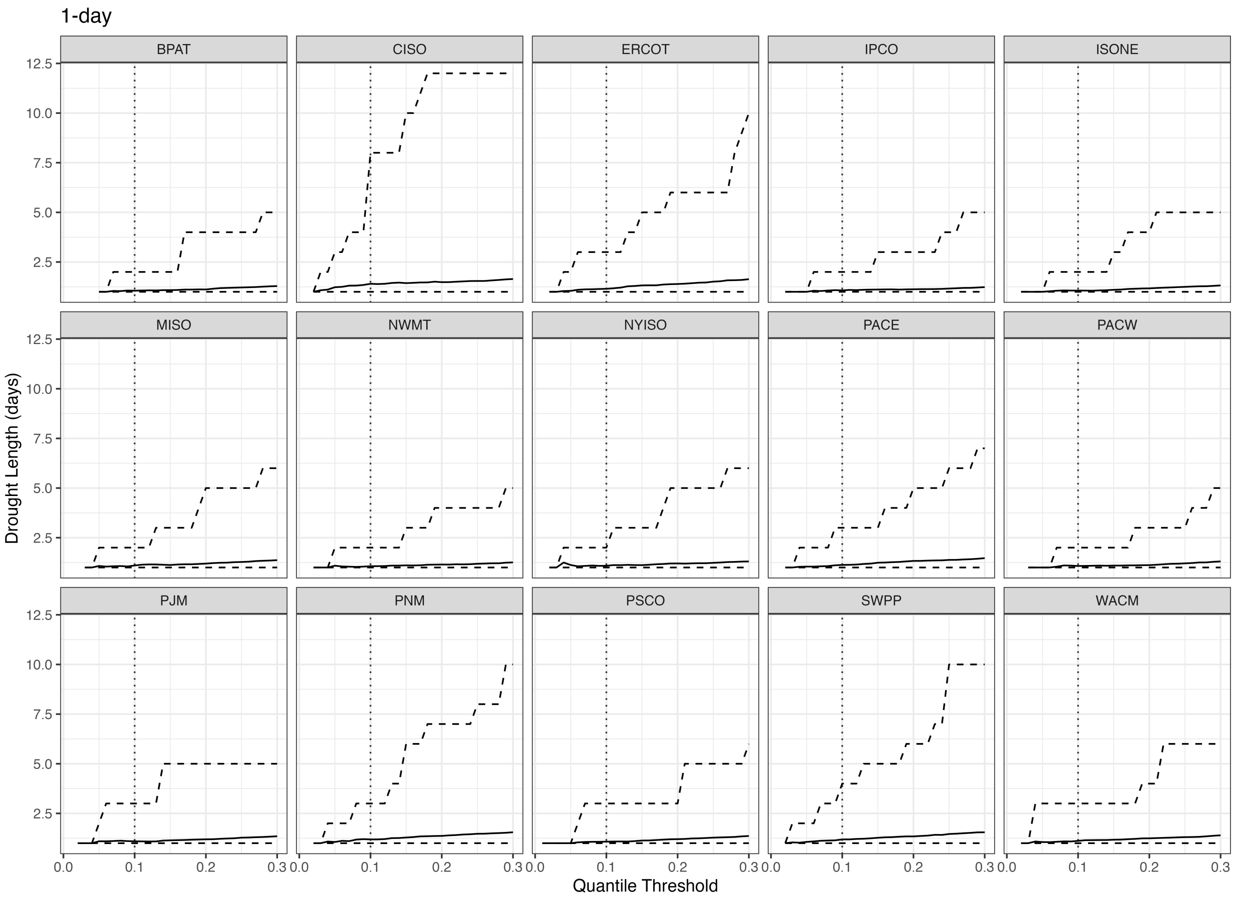

Figure A.7: Sensitivity analysis for drought duration. The dashed lines show the min and max duration and the solid line is the average duration.

Figure A.8 shows a sensitivity analysis of compound WS drought magnitude by changing the percentile threshold for the 1-day time scale. The dashed lines show the min and max magnitude and the solid line is the average magnitude.

Figure A.9 shows the seasonality of 1-day drought frequency defined using a fixed threshold, as opposed to a moving threshold based on time of the year. There is strong seasonality exhibited in many BAs (eg. CISO, PACW) corresponding to periods where wind and solar are both

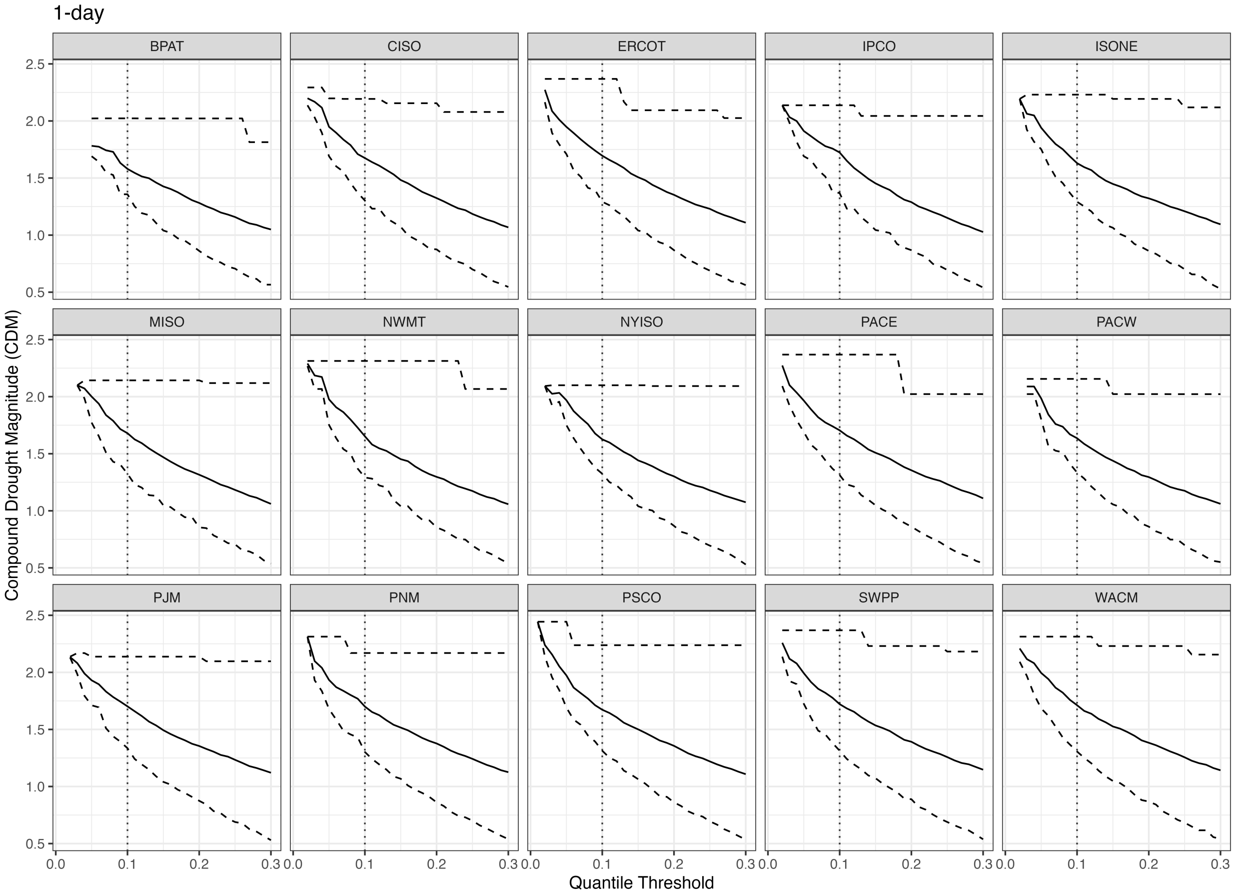

Figure A.8: Sensitivity analysis for drought magnitude. The dashed lines show the min and max magnitude and the solid line is the average magnitude.

climatologically low.

Figure A.9: Average number of droughts per month defined using a fixed 10th percentile threshold. Note the y axis is different for each panel.